Discovery Nature

To Cite:
Umayah OS, Merrious OO, Emmanuel CO. Application of geophysical in evaluation of aquifer potential and vulnerability at Ughelli and its environs, delta sate Nigeria. *Discovery Nature* 2025; 2: e7dn3109
doi: https://doi.org/10.54905/disssi.v2i4.e7dn3109

Author Affiliation:
[1]Department of Physics, Faculty of Science, Abraka, Delta State University, Abraka, Nigeria

[*]**Corresponding Author**
Department of Physics, Faculty of Science, Abraka, Delta State University, Abraka, Nigeria
Email: otiteu@delsu.edu.ng / otitestarumuayah@gmail.com

Peer-Review History
Received: 07 March 2025
Reviewed & Revised: 18/March/2025 to 25/June/2025
Accepted: 01 July 2025
Published: 12 July 2025

Peer-Review Model
External peer-review was done through double-blind method.

Discovery Nature
pISSN 2319-5703; eISSN 2319-5711

Application of geophysical in evaluation of aquifer potential and vulnerability at Ughelli and its environs, delta sate Nigeria

Umayah Otitie Star[1]*, Merrious Oviri Ofimola[1], Emmanuel Chukwuemeka Okolie[1]

ABSTRACT

In the Niger Delta region of Nigeria, specifically in Ughelli and its surrounding areas, the VES geophysical method was employed to investigate groundwater potential and aquifer vulnerability. The Schlumberger array, utilized for the conduction of Vertical Electrical Sounding (VES), facilitated the selection of ten specific VES locations. The maximum spacing of the current electrodes (AB/2) reached 100 meters while utilizing the ABEM Terrameter SAS 1000. Data interpretation was carried out using IX1D software, which incorporated a partial curve matching technique alongside a computer iteration method. The analysis of the estimated parameters revealed ranges for longitudinal conductance (S) between 9 and 379.09, transverse unit resistance (*Tr*) between 2.79Ω/m² and 5344.14Ω/m², longitudinal resistance (ϱL) from 1.88 Ω-m to 544.8 Ω-m, and transverse resistance values ranging from 2 to 538.74. The investigation identified the existence of four to five distinct layers of curve types, with curve HK and HKA being the predominant types. Analysis of the VES layers indicated a range of four to five layers. Furthermore, the findings from the Tr values demonstrated that the area surrounding VES 9 exhibited greater groundwater potential in comparison to other regions within the study area.

Keywords: Resistivity, Depth, Thickness, Curve type

1. INTRODUCTION

Freshwater is relatively evenly distributed across the globe, with approximately 98% of it residing underground. This underground source provides a consistent and reliable supply, typically not subject to complete depletion under normal circumstances, unlike surface water. Groundwater is the most widely utilized source of drinking water worldwide, as it is readily accessible to users and often more reliable than surface water sources (Eyankware et al., 2022). However, various issues are contributing to the global decline in water resource quality. A significant factor influencing water quality is human activity, especially within the studied region.

Many scientific fields, including microbiology, biochemistry, and geology, have been actively engaged in examining the gradual decline in water quality. A comprehensive understanding of the hydrogeological and geological characteristics of the study area is essential for accurate interpretation. Subsurface features associated with geological variability in a model can influence various aspects, including local and regional water cycles; areas of recharge and discharge; hydrogeological properties such as hydraulic conductivity and porosity; and the movement of water into aquifers (Eyankware et al., 2022; Eyankware and Aleke, 2021). In many cases, thorough geophysical investigations are essential prior to the extraction of groundwater to gain insight into subsurface lithology and aquifer zones, including fractures, faults, and joints, which contribute positively to both groundwater storage and quality. However, the effectiveness of geophysical studies and traditional approaches like geostatistical and numerical modeling is often limited due to inadequate data coverage for the effective development and management of groundwater resources (Eyankware et al. 2022). Research conducted by Eyankware et al. (2022), Umayah and Eyankware (2022), & Eyankware and Aleke (2021), and various other scholars has thoroughly investigated the evaluation of groundwater potential and aquifer vulnerability in typical basement complex terrains. These studies typically examined hydrogeological and geoelectrical characteristics such as transmissivity, hydraulic conductance, aquifer thickness, and resistivity in isolation to assess groundwater potential. Recently, the utilization of geophysical methods for analyzing aquifer vulnerability has gained traction. Geophysical techniques, especially those that incorporate electric resistivity, are valuable for estimating building foundations, mapping groundwater distribution, and assessing aquifer susceptibility, among other applications. Eyankware et al. (2022) and Eyankware and Aleke (2021) conducted groundwater studies utilizing geophysical instruments (Eyankware and Umayah, 2022). They noted that various geophysical methods, including electrical resistivity, seismic analysis, gravity measurements, and ground-penetrating radar, are applicable for the exploration of groundwater resources. The electrical resistivity method, which employs a Schlumberger electrode array and vertical electrical sounding, allows for the investigate on of both the depth and spatial distribution of diverse hydro-lithostratigraphic units. Because these geophysical techniques are often non-invasive and capable of covering extensive areas, they can produce densely populated databases. Geophysical data serves as a valuable tool in identifying hydrogeological properties, including the boundary conditions of base aquifers, which are essential for groundwater modeling (Opara, et al., 2025; Umayah and Eyankware, 2022). However, the effectiveness of geophysical methods is constrained and influenced by the characteristics of the physical feature being studied. The scope of the investigation, along with both lateral and vertical resolution, dictates the extent to which the acquisition strategy can probe into the subsurface. Integrating hydrogeological and geophysical datasets during aquifer characterization showcases the unique benefits of each approach, as this synergy can lead to a more accurate depiction of the subsurface (Akinseye, et al., 2023; Opara, et al., 2023).

Location, climate, and Topography

The area under study is situated between the latitudes of 5˚31′ - 5˚35′N and the longitudes of 6˚2′ - 6˚6′E, as illustrated in Fig. 1. This region is characterized as a typical coastal plain, featuring low-lying terrain that gradually slopes down towards the Ethiopian River. The climate here is equatorial, marked by high temperatures ranging from 23 to 37°C and humidity levels between 50 to 70%. The months from November to February are identified as the dry season, while March signals the onset of the wet season, which reaches its maximum intensity in July and October. Over a six-year timeframe from 2000 to 2005, the average annual rainfall recorded in the study area amounted to 3317.8 mm (Irwin and Oghenevwede, 2014). The predominant types of vegetation consist of secondary forests and agricultural lands, which have supplanted most of the devastated rainforest. However, a dense and marshy primary forest still lines the riverbanks.

Geology and hydrogeology of the study area

The region falls within the Niger Delta Basin, which is a prominent and thoroughly examined petroleum province. In essence, it is widely accepted that the rift between the African and South American tectonic plates during the Jurassic Period resulted in the development of this aulacogen-type basin. This subsequent depression was filled by a series of marine transgressions, regressions, and delta formations, the latest being the existing Niger delta. The sedimentary fill of the basin consists of three distinct layers, primarily the Akata Formation, the Agbada Formation (both dating from the Eocene to the present), and the Benin Formation, which ranges from the Miocene to the present.

However, the more recent Holocene strata of the Sombreiro-Warri Deltaic Plain, the Mangrove Swamp, and the Freshwater Swamp wetlands conceal the Benin Formation located to the west and directly south of Abraka. These layers can only be differentiated based

on the physiographic landscapes in which they occur; they lack formal geological designations since they are widely regarded as contemporary extensions of the Benin Formation.

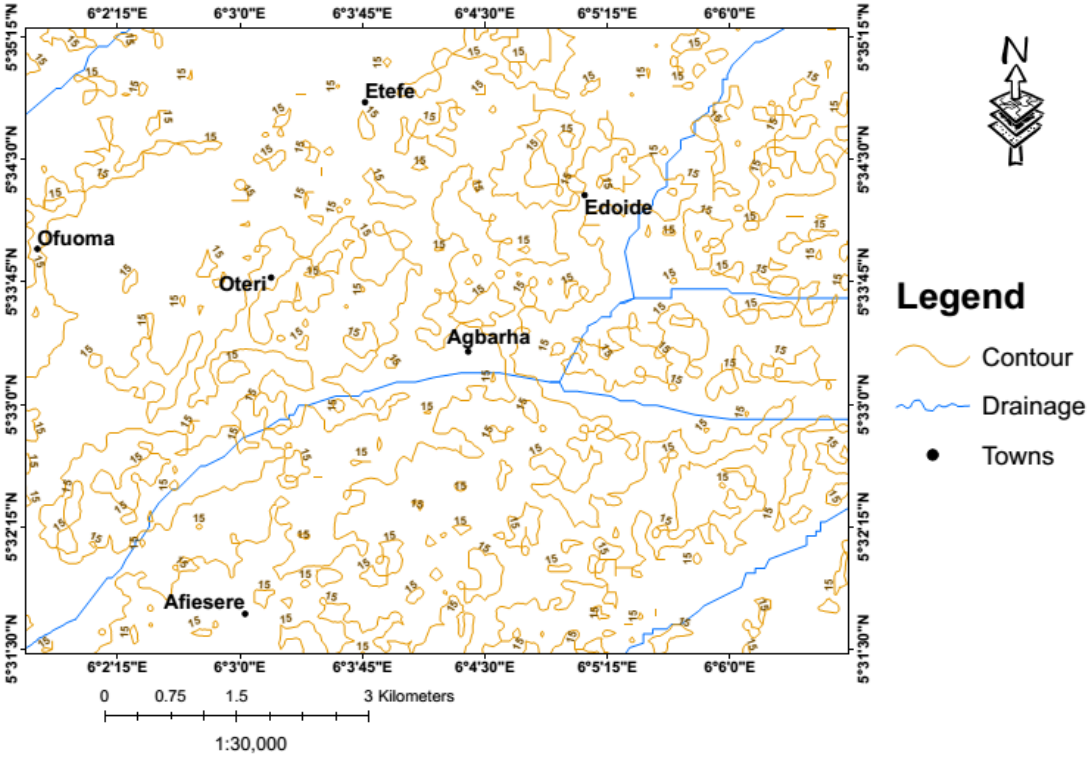

Fig. 1: Location Map of the study area.

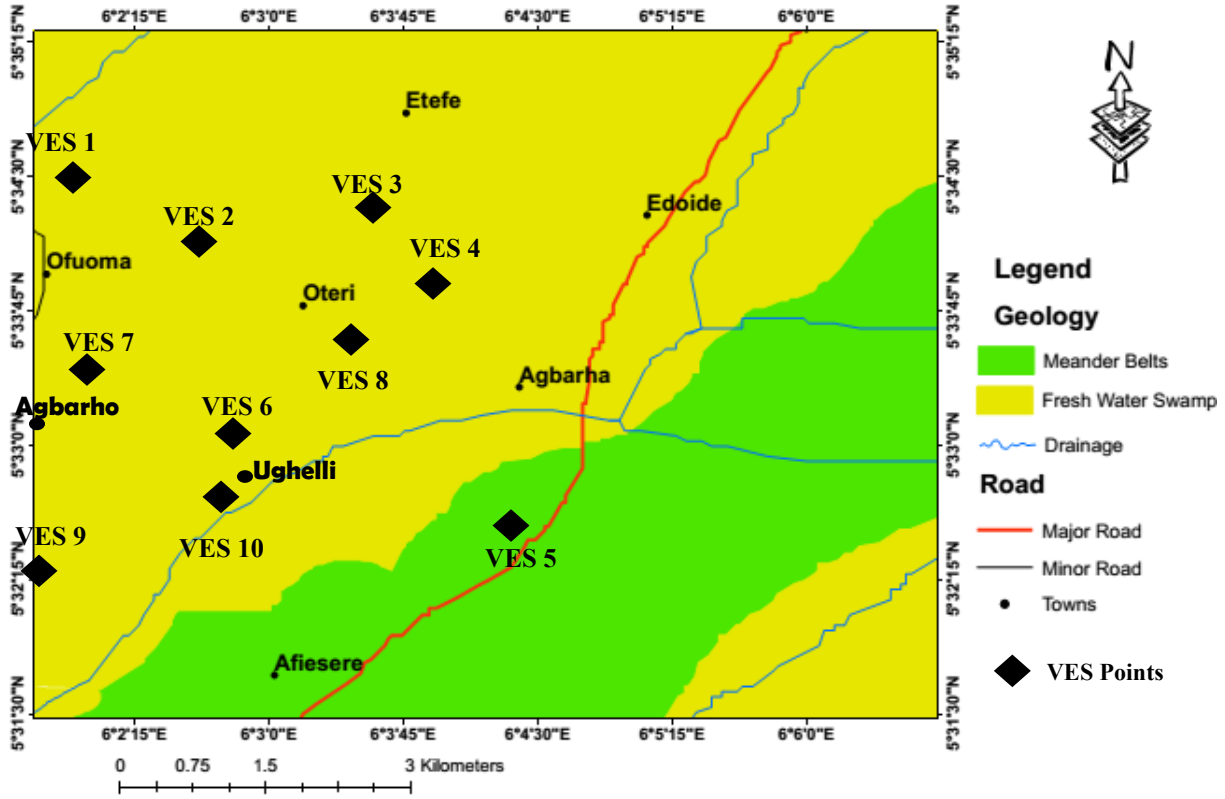

Fig.2: Geological Map of the study area.

The deposits of the Sombreiro-Warri Deltaic Plain occupy the southern section of the Abraka region, whereas the Benin Formation outcrop is situated in the northern area. The Ethiope River, recognized as the most important physiographic characteristic of the region, primarily traverses the outcrop of the Benin Formation. The spatial arrangement of these delta top deposits aligns to some extent with the related physiographic divisions illustrated in Figure 2. In the Abraka vicinity, the Benin Formation is consistently covered by a reddish-brown ferruginized regolith, which generally has a thickness of at least 2 meters. This phenomenon is prominently observable at two specific points along the Abraka-Ugo route. One of these sites is a substantial borrow pit located just before the Ethiopian River bridge, where materials for construction and roadworks are extracted. The other site can be found at the railroad crossing near the flyover on the Abraka-Ugo Road. At both locations, the formation is extensive and significantly eroded.

2. MATERIALS AND METHODS

In the study area, a total of ten (10) Vertical Electrical Soundings (VES) were conducted utilizing an OHMEGA Terrameter along with its accessories. Each VES profile utilized a Schlumberger electrode array, characterized by a maximum half current (AB/2) electrode spacing of 100 meters and a maximum half potential (MN/2) electrode spacing of 5 meters. Spatial distribution maps for S, Tr, L, and pt were generated employing the Surfer program. The field measurements obtained were converted into apparent resistivity (a) values using the specified equation (1), detailed as follows:

$$\pi\left(\frac{\left(\frac{AB}{2}\right)-\left(\frac{MN}{2}\right)}{MN}\right)\Delta V/I \qquad (1)$$

The apparent resistivity measurements were graphed against the current electrode spacing (AB/2) to generate the geoelectrical curves. The IX1D program facilitated the creation of accurate sound curves, assisting in the data processing efforts. The geoelectrical sections, derived from the information obtained through the sounding curves, were instrumental in assessing the thickness of the aquifer. Lithologies corresponding to the geoelectric section were identified using charts from Kearey et al., (2002). Additionally, various factors

concerning the interplay of thickness and resistivity within the geoelectric layer are crucial for comprehending the geological model. The characteristics of Dar Zarrouk, specifically the longitudinal (S) and transverse (T) attributes, are derived through

$$S = \frac{h}{p} \quad (2)$$

$$T = hp \quad (3)$$

Using the formula below, we determined the total Longitudinal Unit Conductance (S).
The total longitudinal conductance is equal to the number of layers (n).

$$S = \sum_{i=1}^{n} \frac{h_i}{\rho_i} = \frac{h_i}{\rho_i} + \frac{h_2}{\rho_2} + \cdots + \frac{h_n}{\rho_n} \quad (4)$$

For the equation below, the Transverse Unit Resistance (*Tr*) was determined.
The total resistance of the transverse unit is

$$Tr = \sum_{i=1}^{n} h_i\rho_i = h_i\rho_i + h_2\rho_2 + \cdots + h_n\rho_n \quad 8 \quad (5)$$

Below is the average longitudinal resistance for a given VES points

$$\rho_L = \frac{H}{S} = \frac{\sum_{i=1}^{n} h_i}{\sum_{i=1}^{n} \frac{h_i}{\rho_i}} \quad (6)$$

The equation is used to calculate the Transverse Resistance for a particular VES curve.

$$\rho_t = \frac{T}{H} = \frac{\sum_{i=1}^{n} h_i\rho_i}{\sum_{i=1}^{n} h_I} \quad (7)$$

3. RESULTS AND DISCUSSION

VES survey

Table 1 provides a summary of the analyzed VES survey results. The VES findings indicate that the geoelectric layers vary from three to six in number, exhibiting distinct intra-facies and inter-facies variations, as illustrated in Table 1 Fig 3(a & b).

Table 1: Results of interpreted VES data

VES	LAYES	RESISTIVITY (ΩM)	THIICKNESS M	DEPTH (M)	INFERRED LITHOLOGY	CURVES
1	1	2112.7	0.65	0.65	Top soil	
	2	301.31	4.42	4.07	Fine grain sand	HK
	3	28.68	5.37	10.44	Clay	
	4	707.4	18.52	28.95	Fine grain sand	
	5	2.18			Clay	
2	1	345.97	2.6	2.6	Top soil	
	2	118.97	11.3	13.90	Clayey sand	QH
	3	293.0	12.518	26.40	Fine grain sand	
	4	39.34	42.25	68.70	Clay	
	5	379.6			Fine grain sand	
3	1	1494.8	2.22	2.22	Top soil	
	2	378.1	12.60	14.79	Fine grain sand	

	3	55.89	50.00	64.80	Clay	H
	4	257.1			Fine grain sand	
4	1	422.2	3.07	3.07	Top soil	
	2	27.587	3.07	6.14	Clay	
	3	45.65	0.91	7.06	Clay	
	4	13.21	17.34	24.41	Clay	HKH
	5	75.21			Clay	
5	1	102.8	1.72	1.72.	Top soil	
	2	45.89	13.75	15.48	Clay	
	3	314.02	32.67	48.15	Fine grain sand	HK
	4	19.418				
6	1	1029.7	3.24	3.24	Top soil	
	2	232.06	6.91	10.16	Fine grain sand	
	3	1562.8	9.41	19.56	Medium grain sand	
	4	19.498	23.86	43.43	Clay	HKA
	5	1730.9			Medium grain sand	
7	1	290.76	0.81	0.81	Top soil	
	2	53.808	7.58	3.39	Clay	
	3	68.88	3.27	6.67	Clay	
	4	164.39	17.42	34.09	Clayey sand	
	5	28.138	39.15	63.24	Clay	
	6	303.10			Fine grain sand	
8	1	404.59	1.67	1.67	Top soil	
	2	41.104	7.988	9.65	Clay	
	3	347.39	10.58	20.2	Fine grain sand	HKA
	4	8.0168	31.46	51.7	Clay	
	5	3191.0			Coarse sand	
9	1	147.48	3.49	3.49	Top soil	
	2	29.2862	0.44	3.94	Clay	HK
	3	352.60	13.66	17.61	Fine grain sand	
	4	7.7037			Clay	
10	1	306.50	0.91	0.91	Top soil	
	2	168.44	1.88	2.79	Clay sand	
	3	94.58	42.60	45.39	Clay sand	Q
	4	61.710			Clay sand	

Table 2: Results of secondary geoelectric parameters

VES Points	Longitudinal Conductance (S)	Transverse Unit Resistance (Ti)	Longitudinal Resistance (ρL)	Transverse Resistivity (ρt)
1	301.31	5.07	4.42	2
2	336.00		66.09	5
3	378.09		12.57	4
4	1.45	1743.90	544.8	538.74
5	314.02	48.14	46.42	3
6	232.06	10.15	6.91	2
7	233.74		62.43	4 and 6

8	347.39	20.24	18.57	3
9	0.07	5344.14	212.56	529.44
10	169.44	2.79	1.88	2
Min.	0.07	2.79	1.88	2
Max.	378.09	5344.14	544.8	538.74
Aver.	224.31	1391.26	126.942	148.17

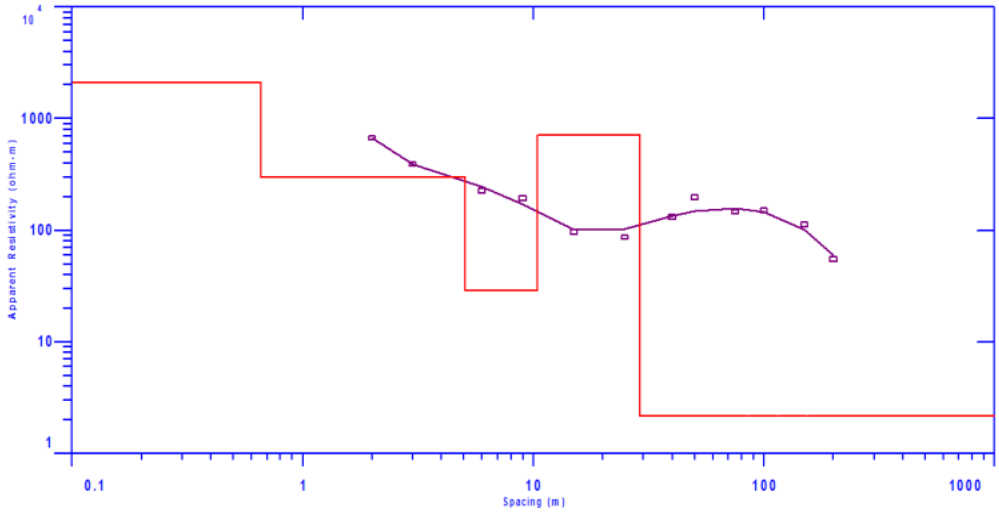

Fig. 3a: Graph of VES 1- Ehwerhe Agbarho

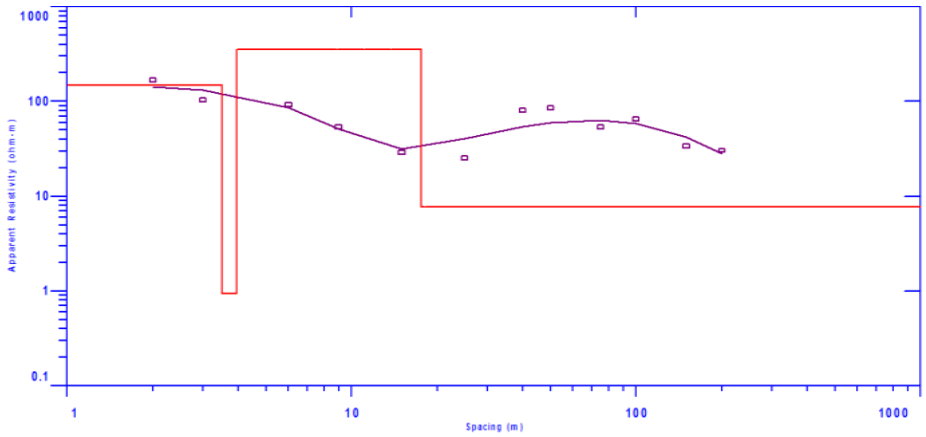

Fig. 3b: Graph of VES 8- Agbarho

The capacity of an earth medium to provide protection is defined by its effectiveness in decelerating and halting the movement of percolating fluids. This parameter is commonly used to assess the susceptibility of an aquifer to pollution. As the overloaded unit of a geological formation—such as clay, shale, and compact sandstone—increases, the protective potential of the area also enhances. For this study, S values were derived using equation 4, yielding a range from 0.07 at VES location 9 to 379.09 at VES location 3, with an average calculated at 224.31, as detailed in Table 2. Analysis of Table 3 indicated that VES locations 1, 2, 3, 4, 5, 6, 7, 8, and 10 were classified in the excellent category, suggesting that the aquifers in these areas are regarded as free from surface contamination, specifically the infiltration of leachate from above. This protection is likely due to the presence of clay layers overlying the subsurface rock formations in the study region (Fig. 4). Conversely, VES locations 4 and 9 were categorized as moderate, indicating that the water-bearing units in these locations are somewhat susceptible to surface contamination.

Table 3: Showing aquifer protective capacity rating

Rating	Remarks	Remarks
> 10	Excellent	VES 1, 2, 3, 4, 5, 6, 7, 8 and 10
5-10	Very good	
0.2-4.9	Moderate	VES 4, and 9
0.1-0.19	Weak	
<0.1	Poor	

Transverse unit resistance (*Tr*)

This method serves to identify the most productive regions of groundwater potential for hydrogeological research (Eyankware et al. 2022). In this study, *Tr* was derived using equation 5. The characteristics of the conducting layers are influenced by longitudinal conductance, whereas transverse resistance affects the properties of the resistive layers. Furthermore, Tr exhibits a significant correlation with transmissivity (Eyankware and Aleke, 2021). Deduction from Table 2, showed *Tr* value ranges from 2.79Ω/m² at VES location 10 to 5344.14Ω/m² at VES location 9, with an average of 1391.26 Ω/m² as shown in Table 2. It has been noted that the transmissivity of a water-bearing unit is directly related to its transverse unit resistance. Analyzing Table 2 and Figure 5 reveals that the regions surrounding VES location 9 exhibit a significantly higher potential for groundwater compared to other areas within the study region.

Longitudinal Resistance (*ρ*L)

The calculation of ρL was derived from equation 6. According to George (2021), longitudinal resistance is instrumental in assessing the potential infiltration rates of aquiferous units. He further noted that due to the sensitivity of ρL to geological formations, it can be utilized to identify the direction of conductivity with increasing depth. As presented in Table 2, the ρL values were found to vary from 1.88 Ω-m at the VES location to 544.8 Ω-m at VES location 4, yielding an average of 126.942 Ω-m (Fig. 6).

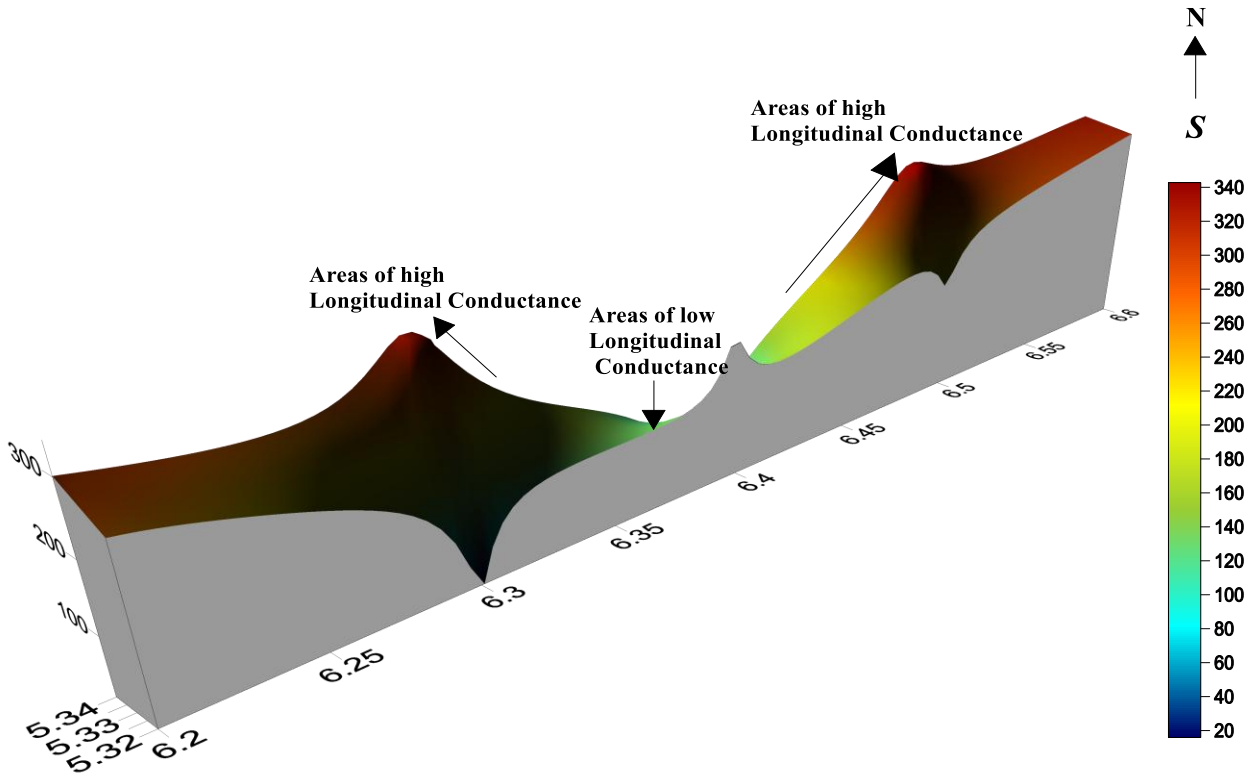

Fig 4: 3D Map of longitudinal conductance of the study area.

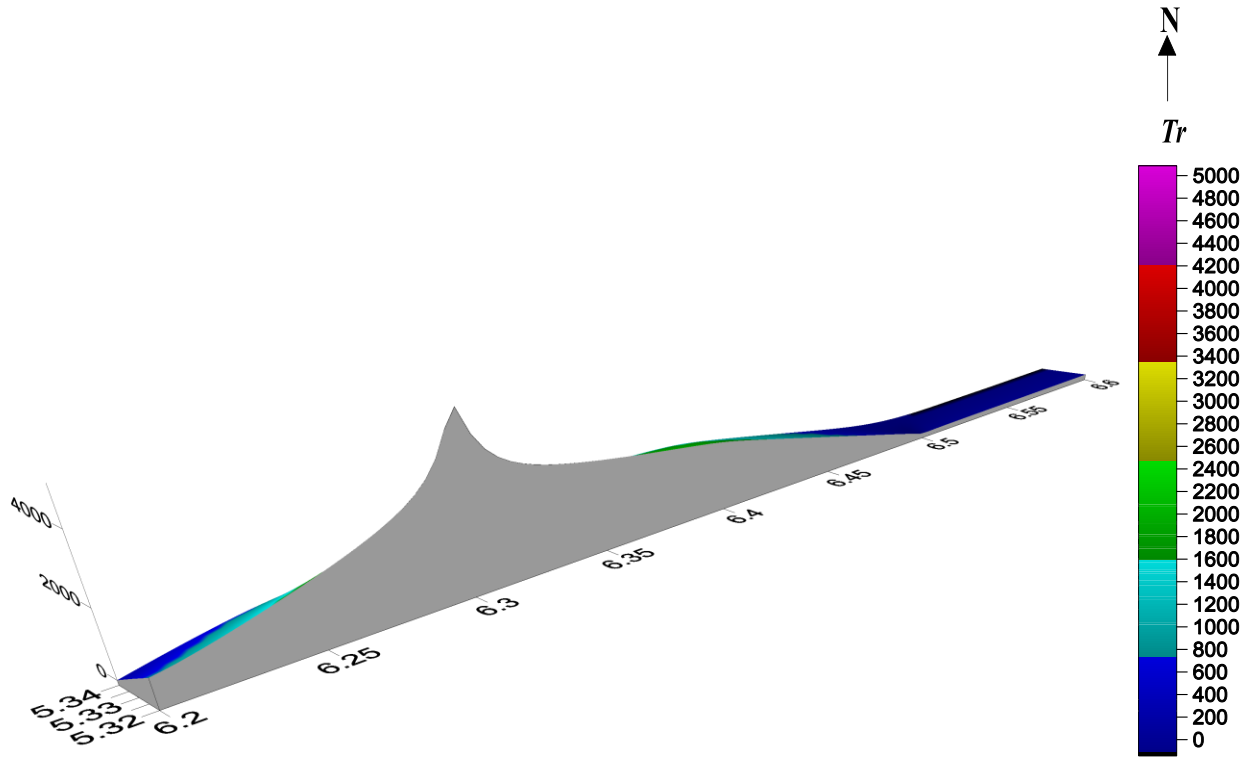

Fig 5: 3D Map of *Tr* of the study area.

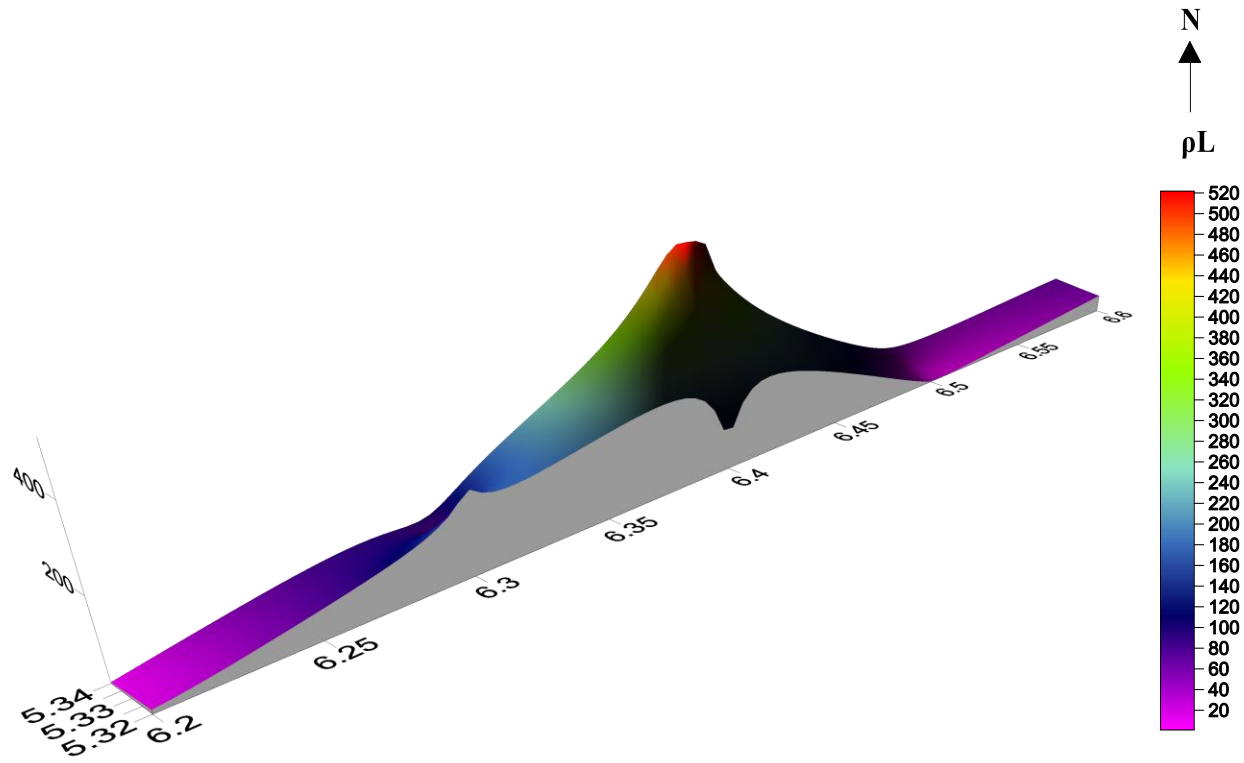

Fig 6: 3D Map of ρL of the study area.

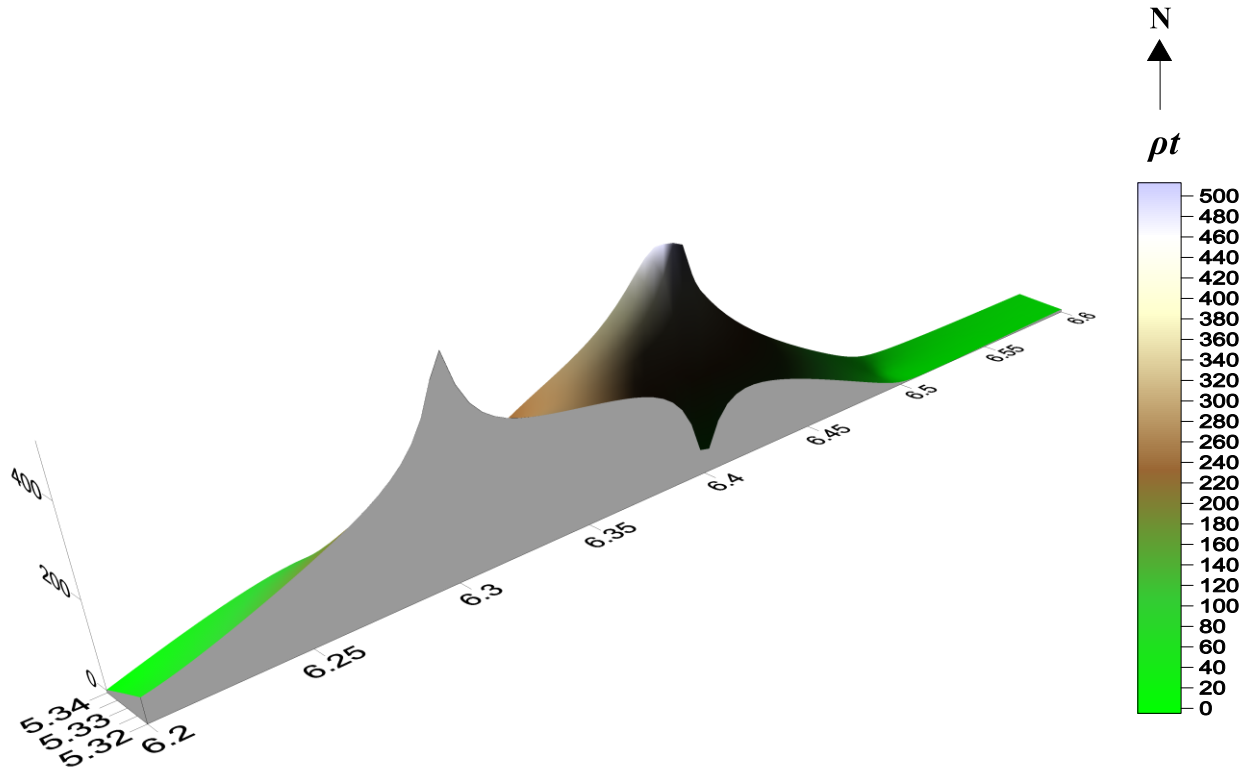

Fig 7: 3D Map of ρt of the study area.

Transverse resistance (ρt)

A key characteristic for identifying regions with promising groundwater potential is the transverse resistance (ρt). Eyankware and Aleke (2021) along with Eyankware et al. (2022) indicate a direct relationship between transverse resistance and transmissivity, suggesting that locations with the highest transverse resistance values are likely to exhibit the highest transmissivity values in their respective aquifers or aquiferous zones. For this study, Equation 7 was applied to calculate the transverse resistance. As illustrated in Table 2, the ϱt values varied from 2 to 538.74, with an average value of 148.17, as detailed in Table 2 (Fig. 7).

Curve type

Based on the deductions from VES, the study area exhibits five distinct curve types: HK, QH, Q, HKA, HKH, and H, as illustrated in Fig. 8. Among these, curves HK and HKA emerged as the most dominant in the area of investigation, as depicted in Fig. 3a and 3b. A related analysis conducted by Eyankware et al. (2022) identified the HK curve as the most frequently occurring type within the Nigerian Niger Delta Basin. Furthermore, Umayah and Eyankware et al., (2022) suggested that the geological variability of the research region could be responsible for the differences observed in curve types.

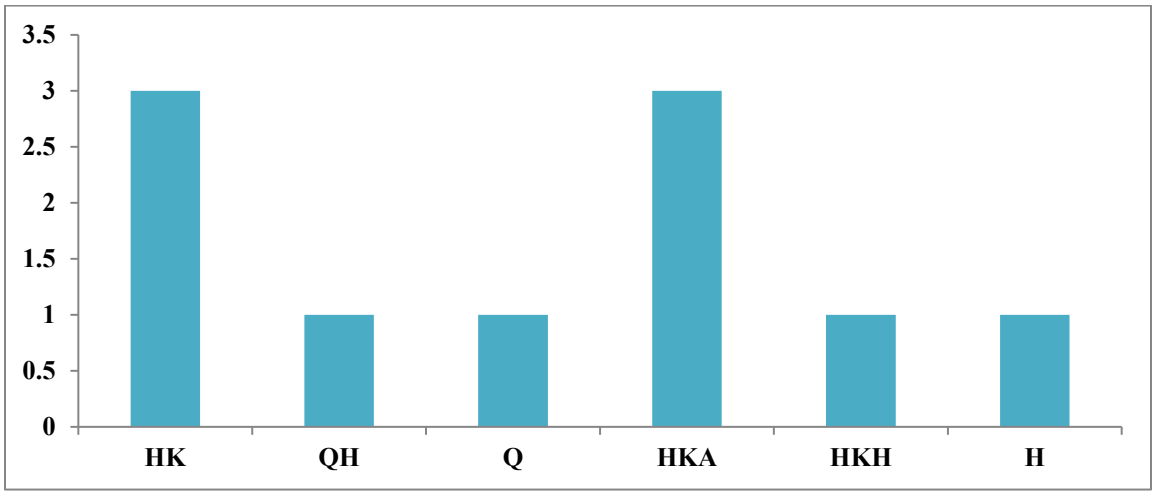

Fig. 8: Plot of occurrence of curve type

4. CONCLUSION

In order to assess the potential of the aquifer, a geophysical study employing electrical resistivity techniques was carried out in Ughelli and its vicinity within the Niger Delta of Nigeria. The findings align closely with the weathered geological formation of the area, specifically the Asu River Group, and the high transverse resistance values obtained from the geoelectric measurements conducted. When longitudinal conductance values, represented by the Dar-Zarrouk parameter, were analyzed in relation to the aquifer protection capacity ratings, it was evident that the aquifer units exhibited no signs of leachate contamination. Previous research suggests that this condition is attributable to the significant presence of clay-rich soils and topsoil that underlie the study region.

Acknowledgement

None.

Informed consent

Not applicable.

Ethical approval

Not applicable.

Conflicts of interests

The authors declare that there are no conflicts of interests.

Funding

This study has not received any external funding.

Data and materials availability

All data associated with this study are present in the paper.

REFERENCES AND NOTES

1. Akinseye VO, Osisanya WO, Eyankware MO, Korode IA, Ibitoye AT. Application of second-order geoelectric indices in determination of groundwater vulnerability in hard rock terrain in SW. Nigeria. Sustain Water Resour Manag. 2023;9(5).169.
2. Eyankware MO, Akakuru OC, Eyankware OE. Hydrogeophysical delineation of aquifer vulnerability in parts

of Nkalagu area of Abakaliki, se. Nigeria. Sustain Water Resour Manag. 2022;8(1):39.
3. Eyankware MO, Aleke G. Geoelectric investigation to determine fracture zones and aquifer vulnerability in southern Benue Trough southeastern Nigeria. Arab J Geosci 14(22): 2259
4. Eyankware MO, Umayah SO. 1D modeling of aquifer vulnerability and soil corrosivity within the sedimentary terrain in Southern Nigeria, using resistivity method. World News of Natural Science, 2022;41; 33-50
5. Irwin AA, Oghenevwede E. Groundwater conditions and hydrogeochemistry of the shallow Benin Formation aquifer in the vicinity of Abraka, Nigeria. Int J Water Resour Environ Eng [Internet]. 2014;6(1):19–31
6. Kearey P, Brooks M, Hill I. An Introduction to Geophysical Exploration. 2002. Blackwell Science Ltd., Oxford.
7. Opara AI, Edward O-OI, Eyankware MO, Akakuru OC, Oli IC, Udeh HM. Use of geo-electric data in the determination of groundwater potentials and vulnerability mapping in the southern Benue Trough Nigeria. Int J Environ Sci Technol (Tehran). 2023; 20:8975–9000
8. Opara AI, Ireaja AN, Eyankware MO, Urom OO, Ikoro DO, Akakuru OC, Dioha E, Omoko NE. A critical analysis of the comparative techniques of aquifer protective capacity studies in part of Southeastern Nigeria. Int J Energ Water Res. 2025;9(2):653–85.
9. Umayah OS, Eyankware MO. Aquifer evaluation in southern parts of Nigeria fromgeo-electrical derived parameters. World News of Natural Science. 2022; 42:28-43